Supporting information

Low-Dimensional Strategy of Ultra-Fast High- Efficiency Scintillators for X-Ray Imaging under Indoor Light Interference

Haitao Tang[a,#], Shaowei Feng[b,e,#], Qiping Du[c], Yichen Xu[a], Bin Yu[a], Zhenglin Jia[a], Yong Liu[a], Hailin Liu[a], Kunfeng Chen[d,e], Dongfeng Xue[b,e], Qianqian Lin[a,f,*]*

[a] Key Lab of Artificial Micro- and Nano-Structures of Ministry of Education of China, School of Physics and Technology, Wuhan University, Wuhan, Hubei, 430072, China.

[b] Shenzhen Institute for Advanced Study, University of Electronic Science and Technology of China, Shenzhen 518110, China.

[c] China Rare Earth Group Research Institute, Ganzhou, 341000, China.

[d] Institute of Novel Semiconductors, State Key Laboratory of Crystal Materials, Shandong University, Jinan 250100, China.

[e] SIAS, UESTC-JIREOIMD Joint Institute of Rare Earth Optoelectronic Information Materials and Devices, Shenzhen 518110, China.

[f] School of Electrical and Information Engineering, Hubei University of Science and Technology, Xianning 437100, China.

[#] These authors contributed equally.

[*]Correspondence: q.lin@whu.edu.cn (Q.L.) dfxue@uestc.edu.cn (D.X.)

1. Experiment details

Materials: Dimethylformamide (DMF, 99%) and diethylether, (Et_2O, 99.5%) were purchased from Aladdin (Shanghai, China). 1-butyl-1-methylpiperidinium bromide, (BmpipBr, 98%) and Tin(II) bromide ($SnBr_2$, 99%) were purchased from Shanghai Macklin Biochemical Co., Ltd. All of these chemical agents were used without further purification.

$Bmpip_2PbBr_4$ powder Synthesis: $Bmpip_2PbBr_4$ powder was prepared by dissolving 0.1 mmol $PbBr_2$ and 0.4 mmol BmpipBr in 1 ml DMF. $Bmpip_2SnBr_4$ powder were grown by a slow diffusion of Et_2O into DMF solution of precursors at room temperature. Crystals were washed with Et_2O and vacuum-dried.

$Bmpip_2PbBr_4$ single crystals Synthesis: 0.4 mmol $PbBr_2$ and 1.6 mmol BmpipBr were dissolved in 4 mL DMF at room temperature under mixing to generate the $Bmpip_2PbBr_4$ solution. The solution was placed in a clean, smooth glass bottle. Seed crystals were obtained by a slow diffusion of Et_2O into DMF solution of precursors at room temperature. High-quality crystals were selected as seeds for further crystal growth. The $Bmpip_2PbBr_4$ single crystals were grown via gradually decreasing the temperature of the water solution. 0.6 mmol $PbBr_2$ and 2.4 mmol BmpipBr were dissolved in 2.4 mL DMF solution to form saturated precursor solution. To guarantee fully dissolution, the solution was stirred at 60 °C for 1 h. Then, the solution was filtrated and transferred to a clean container with a seed crystal placed on the bottom, which was placed on a stable hot plate and gradually cooled with a rate of 1 °C/h to room temperature. The crystal growth process took ~36 h until large single crystals formed.

Characterization: The crystal structure was evaluated with X-ray diffraction (XRD, D8 Advance X-ray diffractometer). The absorption spectra were measured with a visible-NIR spectrometer (Lambda 1050+ UV/VIS/NIR Spectrometer). Photoluminescence (PL) and radioluminescence spectra were recorded using a Morpho Nova spectrometer. The decay curves were recorded with a time-correlated single-photon counter (PicoQuant GmbH, TimeHarp 260) and excited with a 405 nm picosecond laser (Advanced Laser Diode Systems A.L.S. GmbH, Pilas). The device performance under X-ray irradiation was carried out with a commercially available X-ray tube (SPELLMAN XRB011, tungsten anode, 20 W maximum power output). Photodetectors were placed in a lead shielded box to prevent ionizing radiation leakage

and block the external visible lights. The radiation dose rates were carefully calibrated with a commercial dosimeter (Suhe Instrument Technology Co. LTD, XH-3525). For X-ray imaging, X-rays passed vertically through the object, a black baffle and the scintillator wafer in turn. The black baffle blocks leaked visible light and reduces the influence of light reflected from the object on to the scintillator screen. Finally, a CMOS camera with 1,200×1,200 pixels was utilized to acquire X-ray images. The images of scintillator screens under X-ray irradiation were also collected by this system except that the CMOS camera was replaced by a Canon digital camera to take colour photographs.

2. Supplementary note: MTF measurements

2.1 MTF measurements

Modulation transfer function (MTF) determines the spatial resolution of imaging system and represents the ability to transfer input signal modulation of spatial frequency relative to its output. A MTF value of 1 indicates the perfect detection of a given spatial frequency. Using slanted-edge method to calculate MTF, we took the X-ray images of a sharp edge from a piece of aluminum (thickness: ~1mm). The edge spread function (ESF) was derived by the edge profile, from which we could deduce the line spread function (LSF) by calculating derivative. Finally, the Fourier transform of the LSF defines the MTF, meaning the MTF curves could be calculated as,

$$MTF(\nu) = F\big(LSF(x)\big) = F\frac{dESF(x)}{dx} \tag{S1}$$

where the v is spatial frequency, x is the position of pixels. Due to using different optical system, the position of pixels is defined as follows:

$$x = \frac{N.d}{\beta} \tag{S2}$$

where the N is the ordinal number of pixels in X-ray edge image, d is the pixel size and β is optical magnification[1].

2.2 Luminescence lifetime

The decay curves can be well fitted by double exponential decay kinetics:

$$I = A_1 \exp\left(-\frac{t}{\tau_1}\right) + A_2 \exp\left(-\frac{t}{\tau_2}\right) \tag{S3}$$

Where I is the luminescence intensity, t is the time, τ_1 and τ_2 are the luminescence lifetimes, and A_1 and A_2 are fitting parameters. Based on the τ_1 and τ_2 values, the average lifetime (τ) can be calculated by the $\tau = (A_1\tau_1^2 + A_2\tau_2^2)/(A_1\tau_1 + A_2\tau_2)$ equation.[2]

2.3 PLQY calculation

The PLQY can be calculated by the following formula [1]:

$$\eta = \frac{P_c L_b - P_b L_c}{L_a(L_b - L_c)} \quad \text{(S4)}$$

where L_a, L_b, L_c, P_b, and P_c and are the integral values of L and P for experiments P_1, P_2, and P_3 of Figure S3 respectively.[3]

3. Supplementary figures

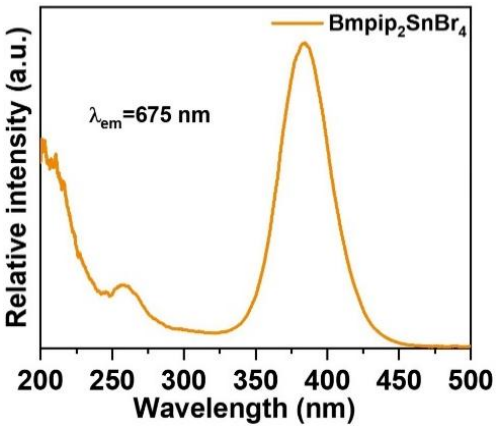

Figure S1. PLE spectra (λ_{em}=675 nm) of $Bmpip_2SnBr_4$.

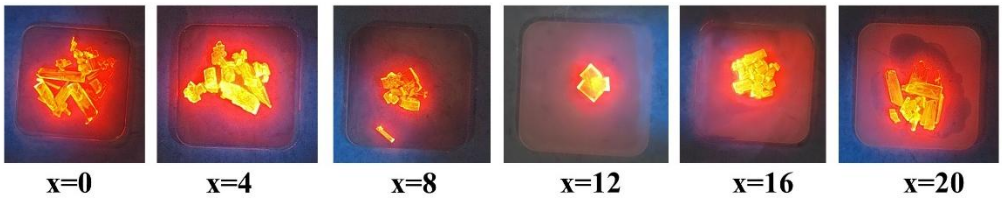

Figure S2. a) Photos of the prepared $Bmpip_2SnBr_4$: x% Cu^+ under 365 nm UV-light.

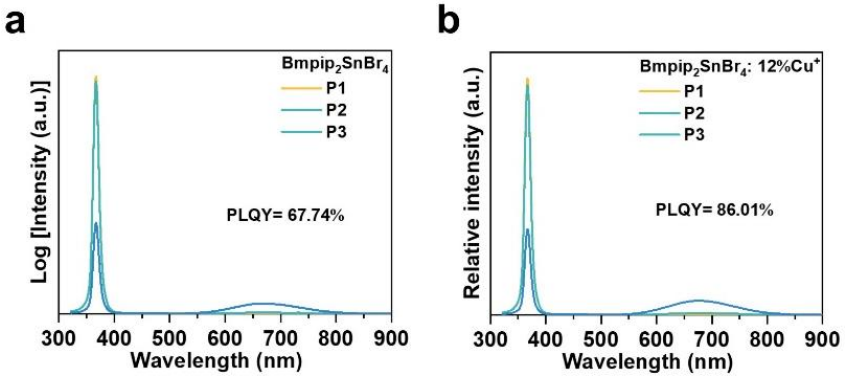

Figure S3. The emission spectra for PLQY measurement in the absence and presence of (a) $Bmpip_2SnBr_4$ and (b) $Bmpip_2SnBr_4$: 12% Cu^+ under 365 nm excitation.

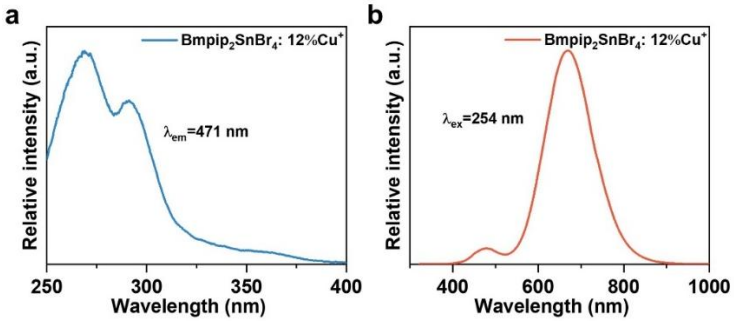

Figure S4. a) PLE (λ_{em}=471 nm) and b) PL (λ_{em}=254 nm) spectra of $Bmpip_2SnBr_4$: 12% Cu^+ single crystals.

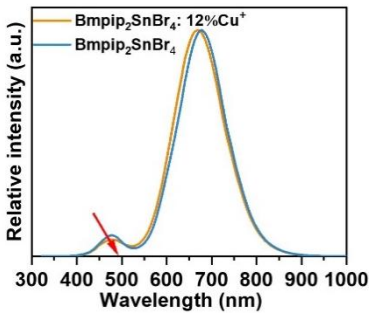

Figure S5. Normalized steady-state PL spectra under 254 nm excitation for $Bmpip_2SnBr_4$: 12%Cu^+ and $Bmpip_2SnBr_4$.

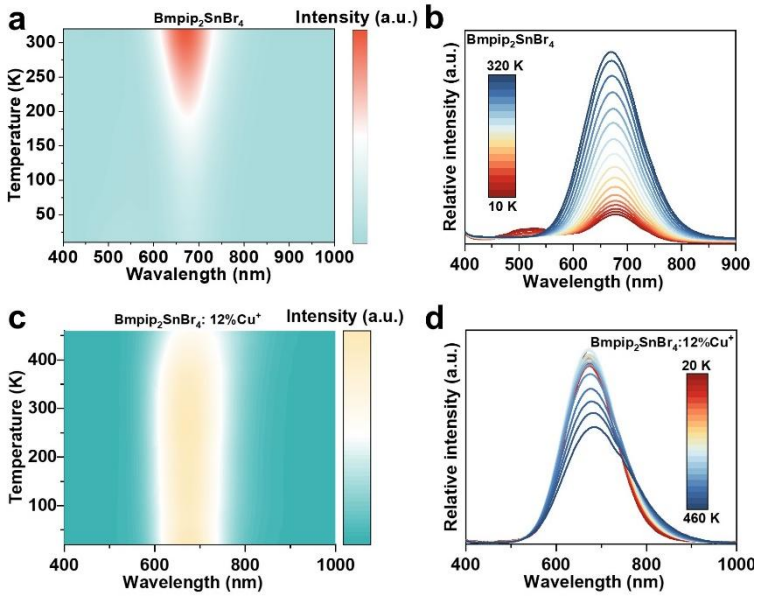

Figure S6. a, b) Temperature-dependent normalized steady-state PL spectra under 365 nm excitation for $Bmpip_2SnBr_4$ crystals. c, d) Temperature-dependent normalized steady-state PL spectra under 365 nm excitation for $Bmpip_2SnBr_4$: 12% Cu^+ crystals.

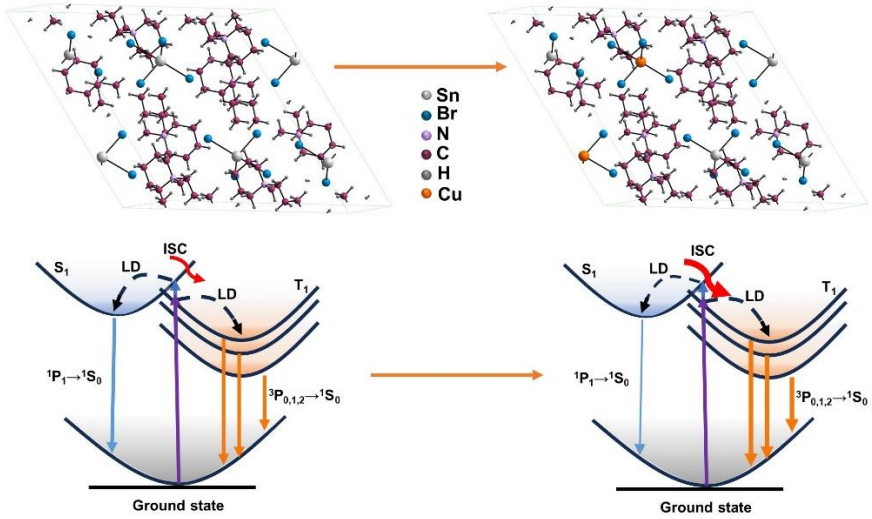

Figure S7. Coordinate diagram to illustrate the luminescence process OF $Bmpip_2SnBr_4$ and $Bmpip_2SnBr_4$: 12%Cu^+.

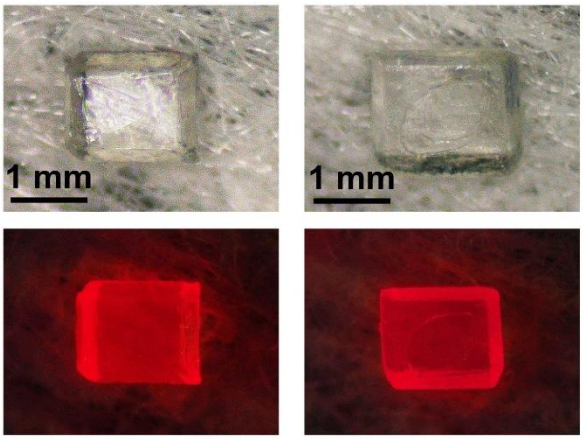

Figure S8. Photos of the prepared $Bmpip_2SnBr_4$: 12% Cu^+ Seed crystals under room- and UV-light.

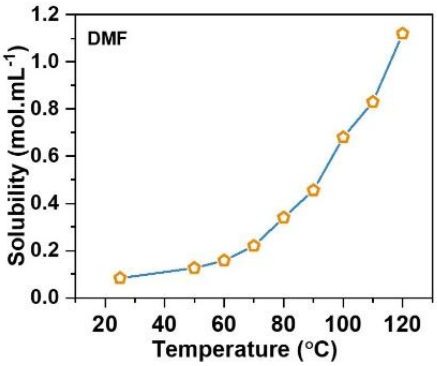

Figure S9. a) Temperature-dependent solubility of $Bmpip_2SnBr_4$: 12% Cu^+ in DMF.

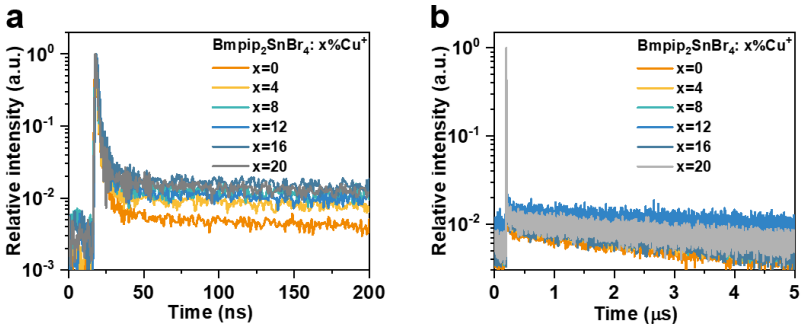

Figure S10. PL decay curve of $Bmpip_2SnBr_4$: x% Cu^+.

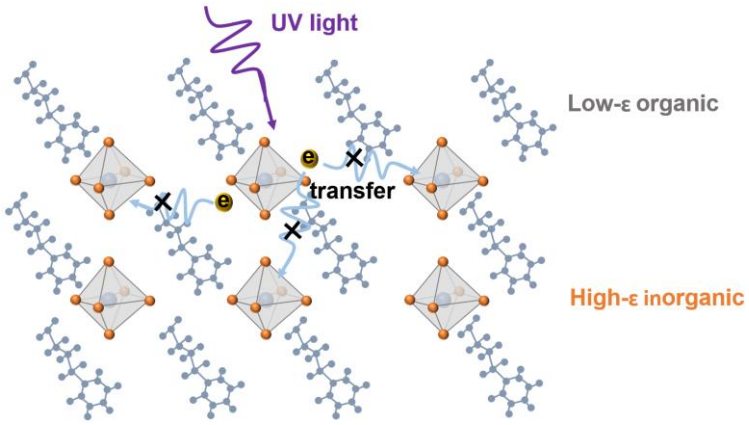

Figure S11. Crystal structures of perovskite with multi-quantum well structure.

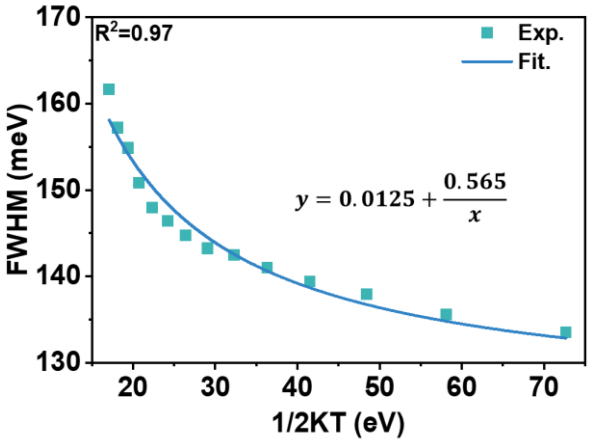

Figure S12. FWHM of the fitting curves of $Bmpip_2SnBr_4$: 12% Cu^+ single crystal.

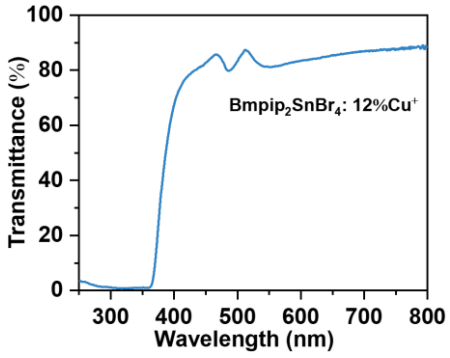

Figure S13. The UV–vis transmittance spectrum of $Bmpip_2SnBr_4$: 12% Cu^+ single crystal.

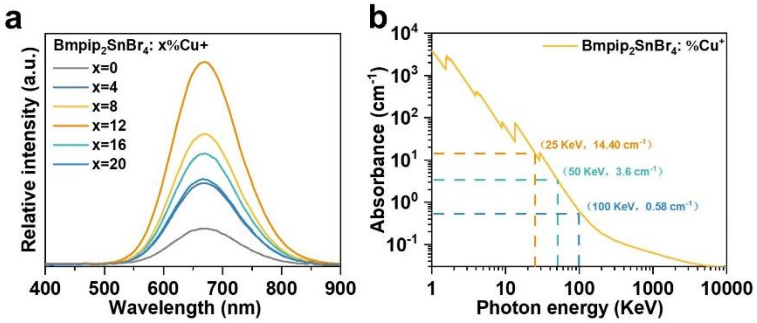

Figure S14. a) RL spectra of $Bmpip_2SnBr_4$: x% Cu^+. b) The absorption coefficient for X-ray of $Bmpip_2SnBr_4$: 12% Cu^+ single crystals as a function of photon energy.

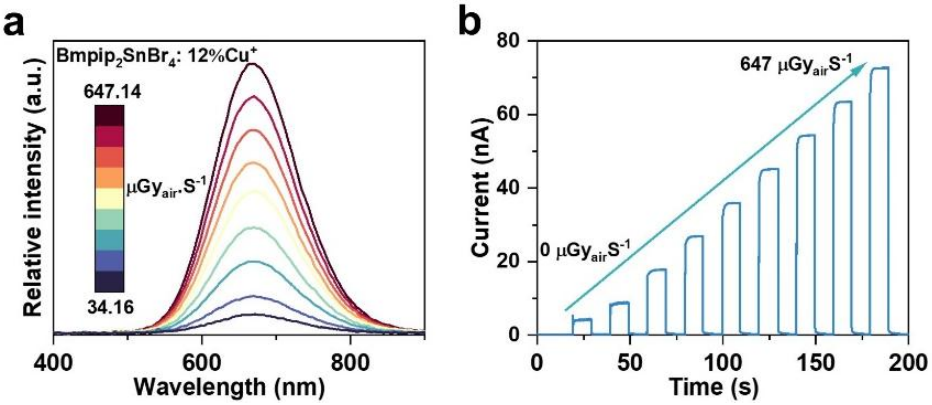

Figure S15. a) RL spectra and b) X-ray response of $Bmpip_2SnBr_4$: 12% Cu^+ single crystals with variable dose rates from 0 to 647 $\mu Gy_{air}s^{-1}$.

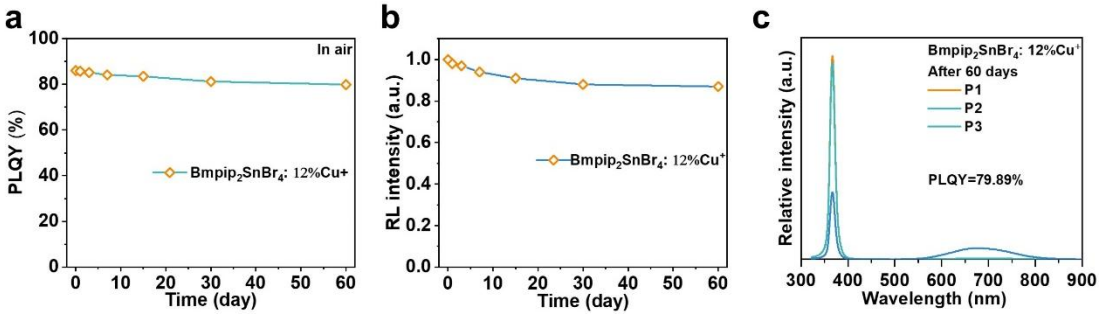

Figure S16. a) PLQY and b) RL intensity of $Bmpip_2SnBr_4$: 12% Cu^+ for prolonged recorded time. c) The emission spectra for PLQY measurement in the absence and presence of $Bmpip_2SnBr_4$: 12% Cu^+ after 60 days. The samples were stored in a nitrogen (N_2) atmosphere for protection.

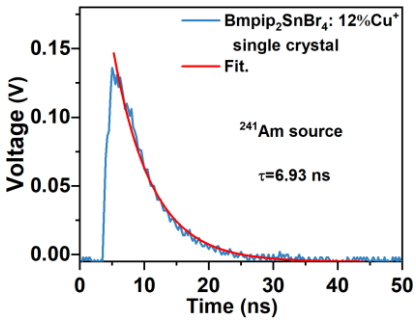

Figure S17 Single pulse signal of $Bmpip_2SnBr_4$: 12%Cu^+ single crystal under irradiation of ^{241}Am source. Pulse signals from ^{241}Am and ^{137}Cs collected by the PMT (Hamamatsu R1317-07) were recorded using a digital storage oscilloscope (LeCroy Waverunner 8254).

Table S1. Comparison of reported scintillation properties of metal halide perovskites.

Material	luminescence decay time (ns)	scintillation light yield photons MeV^{-1}	ref
BGO	100	10600	4
CsI	790	57000	5
$LaBr_3$	17	73000	6
LYSO	41	34000	7
SrI_2	1200	90000	8
YAG	100	25000	9
GAGG	87	50000	10
$CsPbBr_3$ QDs	44.6	21000	11
PEA_2PbBr_4	10.3	22000	12
Cs_2ZrCl_6	15830	94190	13
$Cs_3Cu_2I_5$	19200	79270	14
Cs_2HfCl_6	12290	21700	15
$Cu_4I_6(L1)_2$	58580	30500	16
$(HTPP)_2MnBr_4$	190400	8600	17
$Cs_2AgInCl_6$	16000	39000	18
BaF_2	0.88	1400	19
CuI	0.5	511	19
ZnO: In	0.7	1012	19
CsCl	0.9	896	19
Anthracene	30	100	20
Stilbene	4.5	50	20

EJ-212	2.4	65	20
BC-517L	2	39	20
EJ-309	3.5	80	20
$Bmpip_2SnBr_4$: 12% Cu^+	1.47	57977	This work

References

1 H. Zhang, Z. Yang, M. Zhou, L. Zhao, T. Jiang, H. Yang, X. Yu, J. Qiu, Y. (Michael) Yang, X. Xu, *Adv. Mater.* 2021, **33** 2102529.

2 S. Wang, Q. Sun, B. Devakumar, L. Sun, J. Liang, X. Huang, *RSC Adv.* 2018, **8**, 30191 – 30200.

3 J.C. de Mello, H.F. Wittmann, R.H. Friend, *Adv. Mater.* 1997, **9**, 230 – 232.

4 J. Tang, Shichao Lv, Z. Lin, G. Du, M. Tang, X. Feng, J. Guo, X. Li, J. Chen, L. Wei, J. Qiu, S. Zhou, *J. Mater. Sci. Technol.* 2022, **129**, 173 – 180.

5 L. Guo, S. Liu, D. Chen, S. Zhang, Y. Liu, Z. Zhong, C.M. Falco, *Appl. Surf. Sci.* 2016, **384**, 225 – 229.

6 Y.-Y. Ji, H. Choi, W. Lee, C.-J. Kim, H.-S. Chang, Kun Ho Chung, *IEEE Trans. Nucl. Sci.* 2018, **65**, 2021 – 2028.

7 F. Loignon-Houle, M. Bergeron, C.M. Pepin, S.A. Charlebois, R. Lecomte, *Phys. Med. Biol.* 2017, **62**, 669 – 683.

8 R.H.P. Awater, M.S. Alekhin, D.A. Biner, K.W. Krämer, P. Dorenbos, *J. Lumin.* 2019, **212**, 1 – 4.

9 V.V. Osipov, A.V. Ishchenko, V.A. Shitov, R.N. Maksimov, K.E. Lukyashin, V.V. Platonov, A.N. Orlov, S.N. Osipov, V.V. Yagodin, L.V. Viktorov, B.V. Shulgin, *Opt. Mater.* 2017, **71**, 98 – 102.

10 Y. Zhu, S. Qian, Z. Wang, H. Guo, L. Ma, Z. Wang, Q. Wu, *Opt. Mater.* 2020, **105**, 109964.

11 Q. Chen, J. Wu, X. Ou, B. Huang, J. Almutlaq, A.A. Zhumekenov, X. Guan, S. Han, L. Liang, Z. Yi, J. Li, X. Xie, Y. Wang, Y. Li, D. Fan, D.B.L. Teh, A.H. All, O.F. Mohammed, O.M. Bakr, T. Wu, *Nature*, 2018, **561**, 88 – 93.

12 F. Maddalena, Muhammad Haris Mahyuddin, D. Kowal, M.E. Witkowski, M. Makowski, A. Kuddus, Somnath Mahato, R. Jędrzejewski, W. Drozdowski, C. Dujardin, C. Dang, Muhammad Danang Birowosuto, Lattice Expansion in Rb-Doped Hybrid *Inorg. Chem.* 2023, **62** 8892 – 8902.

13 H. Li, Y. Zhang, M. Zhou, H. Ding, L. Zhao, T. Jiang, H.Y. Yang, F. Zhao, W. Chen, Z. Teng, J. Qiu, X. Yu, Y.M. Yang, X. Xu, *ACS Energy Lett.* 2022, **7**, 2876 – 2883.

14 L. Lian, M. Zheng, W. Zhang, L. Yin, X. Du, P. Zhang, X. Zhang, J. Gao, D. Zhang, L. Gao, G. Niu, H. Song, R. Chen, X. Lan, J. Tang, J. Zhang, *Adv. Sci.* 2020, **7**, 2000195.

15 F. Zhang, Y. Zhou, Z. Chen, X. Niu, H. Wang, M. Jia, J. Xiao, X. Chen, D. Wu, X. Li, Z. Shi, C. Shan, *Laser Photonics Rev.* 2023, **17** 2200848 – 2200848.

16 T. He, Y. Zhou, P. Yuan, J. Yin, L. Gutiérrez-Arzaluz, S. Chen, J.-X. Wang, S. Thomas, H.N. Alshareef, O.M. Bakr, O.F. Mohammed, *ACS Energy Lett.* 2023, **8**, 1362 – 1370.

17 J.-B. Luo, J. Wei, Z.-Z. Zhang, Z.-L. He, D.-B. Kuang, *Angew. Chem., Int. Ed.* 2022, **62**, e202216504.

18 Y. Liu, A. Nag, L. Manna, Z. Xia, *Angew. Chem., Int. Ed.* 2021, **60**, 11592 – 11603.

19 M. Xia, Z. Xie, H. Wang, T. Jin, L. Liu, J. Kang, Z. Sang, X. Yan, B. Wu, H. Hu, J. Tang, G. Niu, *Adv. Mater.* 2023, **35**, 2211769.

20 Inorganic Scintillator Library, Lbl.gov. 2015. https://scintillator.lbl.gov/inorganic-scintillator-library/ (accessed January 6, 2025).